To appear in *Liquid Crystals*
Vol. 00, No. 00, Month 20XX, 1–13

arXiv:1607.02297v1 [cond-mat.soft] 8 Jul 2016

RESEARCH ARTICLE

Modulated nematic structures and chiral symmetry breaking in 2D

Karol Trojanowski, Michał Cieśla and Lech Longa

M. Smoluchowski Institute of Physics, Jagiellonian University, Łojasiewicza 11, 30-248 Kraków, Poland;

(*Received 00 Month 20XX; final version received 00 Month 20XX*)

We have studied the properties of biaxial particles interacting via an anisotropic pair potential, involving second rank quadrupolar and third rank octupolar coupling terms, using Monte Carlo simulation. The particles occupy the sites of a 2D square lattice and the interactions are restricted to nearest neighbours. The system exhibits spontaneous chiral symmetry breaking from an isotropic phase to a chiral modulated nematic phase, composed of ambidextrous chiral domains. When two-fold axes of quadrupolar and octupolar tensors coincide this modulated phase appears to be the ambidextrous cholesteric phase of pitch comparable with a few lattice spacings, which can be regarded as a limiting case of the nematic twist bend phase. The associated phase transition is first-order.

Keywords: modulated liquid crystal structures, chiral symmetry breaking, Monte-Carlo simulations, twist bend nematic, cholesteric phase

1. Introduction

Liquid crystal compounds, such as chemically *achiral* flexible dimers [1–4], trimers [5] and bent-core mesogens [6, 7] with their hybrids [8], can stabilize phases unlike anything recognized before. The most striking observation is one connected with appearance of spontaneous chiral order, where domains of opposite optical activity are created in ordinary isotropic and nematic phases. A new macroscopically chiral nematic state that emerges, known as the twist-bend nematic (N_{TB}), is a helicoidal structure with the director tilted with respect to the helix axis. From the perspective of the purely nematic type of ordering it can be considered as a generalization of the cholesteric phase [9] where the director is orthogonal to helix axis, except for the observation of domains of opposite chirality and a short, nano-scale pitch, apparently spanning only several molecules. This last property is particularly surprising since in the presently known cholesteric phase the pitch is hundreds to thousands of molecules long.

In spite of its importance, the theory that correlates spontaneous chiral symmetry breaking (SCSB) and modulated structures with relevant features of molecular interactions is not yet fully developed and understood. Taking into account that the pitch of N_{TB} is so extremely short, it seems likely that the driving force responsible for its formation is the packing entropy connected with the bent shape (steric dipole) of the constituent molecules [10, 11]. Another possibility would be that chirality could be transmitted via steric interactions emerging from the coupling to chiral conformations [12]. It is this scenario that we would like to discuss, at least partly, in the present paper.

2. Chiral symmetry breaking in non-chiral materials

At the phenomenological level Dozov predicted the existence of N_{TB} as a result of the negative value of the bend elastic constant K_3 in the nematic phase [13]. Since the resulting spontaneous bend

cannot be extended globally the uniform nematic phase would become unstable to the formation of a modulated phase, which could be either chiral N_{TB}, or nonchiral nematic splay-bend (N_{SB}). A possible explanation of the sign change of the bend elastic constant is to assume that spontaneous local bend deformations of the nematic director couple with emerging modulated polar order via the so called flexoelectric effect [14, 15]. Indeed, as follows from a direct calculation such polar order can effectively reduce K_3 and even make it negative [16, 17].

But mesoscopic-level consequences of the fact that the chiral symmetry breaking takes place in the nematic phase are far more reaching. To discuss some of them let us assume that the *primary order parameter* quantifying *local* nematic order in N_{TB} is a full 3×3 second-rank traceless and symmetric alignment tensor field, $\mathbf{Q}(\mathbf{r})$ [9], rather than its director part only. In a standard parametrization $\mathbf{Q}$ can be written as

$$\mathbf{Q} = \frac{q_0}{\sqrt{6}}\left(3\hat{\mathbf{n}}\otimes\hat{\mathbf{n}} - \mathbf{1}\right) + \frac{q_2}{\sqrt{2}}\left(\hat{\mathbf{l}}\otimes\hat{\mathbf{l}} - \hat{\mathbf{m}}\otimes\hat{\mathbf{m}}\right), \tag{1}$$

where eigenvectors of $\mathbf{Q}$ are identified with the orthonormal, right-handed tripod $\{\hat{\mathbf{l}}, \hat{\mathbf{m}}, \hat{\mathbf{n}}\}$ of *local* directors, corresponding to the *local* eigenvalues $\lambda_1 = -\frac{q_0}{\sqrt{6}} + \frac{q_2}{\sqrt{2}}$, $\lambda_2 = -\frac{q_0}{\sqrt{6}} - \frac{q_2}{\sqrt{2}}$, $\lambda_3 = -\lambda_1 - \lambda_2 = \sqrt{\frac{2}{3}}q_0$, respectively. When three eigenvalues of $\mathbf{Q}$ are equal, which gives $\mathbf{Q} = 0$, the local structure is an $SO(3)$-symmetric isotropic liquid. If $\mathbf{Q}$ has two degenerate eigenvalues the local anisotropy is uniaxial, and biaxial if all three eigenvalues are distinct. These properties can be expressed using inequality between traces of $\mathbf{Q}^2$ and $\mathbf{Q}^3$

$$\mathrm{Tr}(\mathbf{Q}^2)^3 - 6\mathrm{Tr}(\mathbf{Q}^3)^2 \geq 0. \tag{2}$$

The condition (2) becomes a strong inequality for locally biaxial (oblate or prolate) configurations and is fulfilled as equality for the uniaxial ($\mathbf{Q} \neq \mathbf{0}$) and the isotropic ($\mathbf{Q} = \mathbf{0}$) orientational ordering. Excluding local isotropic configurations, the normalized parameter

$$-1 \leq w = \frac{\sqrt{6}\,\mathrm{Tr}\left(\mathbf{Q}^3\right)}{\left[\mathrm{Tr}\left(\mathbf{Q}^2\right)\right]^{\frac{3}{2}}} \leq 1 \tag{3}$$

serves as a scalar measure of how strongly uniaxial/biaxial is *local* nematic order. For purely uniaxial phases w^2 is maximal and equals one while for phases of maximal biaxiality w^2 approaches its minimal value 0 [18].

To link SCSB with the local nematic order a basic observation is that a totally antisymmetric tensor $\varepsilon_{\alpha\beta\gamma}$, proportional to the Levi- Civita tensor ϵ_{ijk}, or equivalently, pseudotensor couplings between basic order parameters (responsible for SCSB) must spontaneously emerge at the transition to the chiral phase. In the lowest order scenarios, in addition to $\mathbf{Q}$, we need at least one more primary order parameter, which can be either a first-rank vector field, say $\mathbf{P}(\mathbf{r})$, [19] or a third-rank tensor field $\mathbf{T}(\mathbf{r})$, invariant with respect to tetrahedral point group symmetry [20, 21], or both [21]. The vector $\mathbf{P}$ could represent *e.g.* mesoscopic polar order of steric and/or electric dipoles, or the wave vector of the modulated structure. Non vanishing tensor $\mathbf{T}$ would imply the presence of long-range octupolar part in third-rank nonlinear dielectric tensor. In intrinsically chiral materials, where cholesteric and blue phases are stabilized, $\mathbf{T}$ and $\mathbf{P}$ fields can be correlated *e.g.* with $L = 3$ and $L = 1$ parts of $\partial_i Q_{j,k}$, respectively. Lubensky and Radzihovsky [21] have argued that all three tensors $\mathbf{P}$, $\mathbf{Q}$ and $\mathbf{T}$ are necessary to correctly account for symmetry breaking mechanisms observed in bent-core systems.

As concerning SCSB, $\mathbf{P}$ and $\mathbf{T}$ can both be used to construct the totally antisymmetric tensors $\varepsilon^{\mathbf{X}}_{\alpha\beta\gamma}$ ($\mathbf{X} = \{\mathbf{P}, \mathbf{T}\}$), that provide a chirality measure for the emerging chiral structure. They are

given by

$$\varepsilon^{\mathbf{P}}_{\alpha\beta\gamma} = P_{[\alpha}(\mathbf{Q}\cdot\mathbf{P})_\beta(\mathbf{Q^2}\cdot\mathbf{P})_{\gamma]} \propto |\mathbf{Q}|^3(\hat{\mathbf{l}}\cdot\mathbf{P})(\hat{\mathbf{m}}\cdot\mathbf{P})(\hat{\mathbf{n}}\cdot\mathbf{P}) \times \sqrt{1-w^2}\ \epsilon_{\alpha\beta\gamma} = \varepsilon_{\mathbf{P}}\,\epsilon_{\alpha\beta\gamma} \tag{4}$$

$$\begin{aligned}\varepsilon^{\mathbf{T}}_{\alpha\beta\gamma} = Q_{[\alpha\mu}(\mathbf{Q^2})_{\beta\nu}T_{\mu\nu\gamma]} \propto |\mathbf{Q}|^3|\mathbf{T}|\Big[2(\hat{\mathbf{l}}\cdot\hat{\mathbf{l}}')^2 + 2(\hat{\mathbf{m}}\cdot\hat{\mathbf{m}}')^2 \\ +2(\hat{\mathbf{n}}\cdot\hat{\mathbf{n}}')^2 - 6\,(\hat{\mathbf{l}}\cdot\hat{\mathbf{l}}')(\hat{\mathbf{m}}\cdot\hat{\mathbf{m}}')(\hat{\mathbf{n}}\cdot\hat{\mathbf{n}}') - 1\Big]\ \sqrt{1-w^2}\ \epsilon_{\alpha\beta\gamma} = \varepsilon_{\mathbf{T}}\,\epsilon_{\alpha\beta\gamma}.\end{aligned} \tag{5}$$

Here [...] denotes antisymmetrization over indices α,β,γ; $\{\hat{\mathbf{l}}',\hat{\mathbf{m}}',\hat{\mathbf{n}}'\}$ is the orthonormal tripod of vectors, parallel to 2-fold rotation axes of the octupolar tensor $\mathbf{T}$; $|\mathbf{Q}| = \sqrt{Q_{\alpha\beta}Q_{\alpha\beta}}$ and $|\mathbf{T}| = \sqrt{T_{\alpha\beta\gamma}T_{\alpha\beta\gamma}}$. In addition we have used an Einstein summation convention for the repeated indices. The primary conclusion from the Eqs. (4,5) is that SCSB in nematics, irrespective of the way it is realized in practise, should stabilize a structure which is described *locally* by the *biaxial* tensor field $\mathbf{Q}$. We should mention that the necessity of considering the full biaxial field $\mathbf{Q}$ for a proper understanding of SCSB, rather than its uniaxial part only, is in line with the observation that all chiral phases of at least intrinsically chiral mesogens are biaxial [22]. For cholesterics of periodicity being of the order of 500 nm this biaxiality can be weak and homogeneous ($w \approx 1$), but it becomes relevant for blue phases, where w being space-dependent, varies between -1 and 1.

The condition that biaxiality of $\mathbf{Q}$ is necessary to induce chiral order is, however, not sufficient. For example, for a vector fields $\mathbf{P}$ to contribute to chirality measure $\varepsilon_{\mathbf{P}}$ we need, in addition, that $\mathbf{P}$ does not belong to a plane spanned by any two vectors of the tripod $\{\hat{\mathbf{l}},\hat{\mathbf{m}},\hat{\mathbf{n}}\}$. From the formulas (4,5) one can further conclude that the coefficients $\varepsilon_{\mathbf{P}}$ and $\varepsilon_{\mathbf{T}}$ measuring sign and 'degree of chirality' for given $\mathbf{Q}$, $\mathbf{P}$ and $\mathbf{T}$ are restricted by inequalities

$$-1 \le \frac{3\sqrt{3}\,\varepsilon_{\mathbf{P}}}{|\mathbf{Q}|^3|\mathbf{P}|^3\sqrt{1-w^2}} \le 1 \tag{6}$$

$$-1 \le \frac{\varepsilon_{\mathbf{T}}}{|\mathbf{Q}|^3|\mathbf{T}|\sqrt{1-w^2}} \le 1. \tag{7}$$

Thus, the extremal value of chirality can be achieved for

$$\mathbf{P} = \frac{|\mathbf{P}|}{\sqrt{3}}(\pm\hat{\mathbf{l}} \pm \hat{\mathbf{m}} \pm \hat{\mathbf{n}}), \tag{8}$$

where odd number of ' $-$ ' signs corresponds to a state from the upper limit in (6) while the remaining combinations of ' $+$ ' and ' $-$ ' signs are states from the lower bound in (6). Likewise, taking 2-fold axes of $\mathbf{Q}$ parallel to 2-fold axes of $\mathbf{T}$

$$\{\hat{\mathbf{l}},\hat{\mathbf{m}},\hat{\mathbf{n}}\} \parallel \{\pm\hat{\mathbf{l}}',\pm\hat{\mathbf{m}}',\pm\hat{\mathbf{n}}'\} \tag{9}$$

gives states satisfying lower bound in (7), while permutation of any two vectors on the right-hand side of (9) corresponds to upper bound states. The allowed choice between ' $+$ ' and ' $-$ ' signs in (9) is such that the handedness of both bases should be the same.

It is likely that for molecular systems exhibiting SCSB both ways of acquiring structural chirality can be important. But except for symmetry classification of spontaneous order [21] only special, separate cases of $\{\mathbf{Q},\mathbf{P}\}$ and $\{\mathbf{Q},\mathbf{T}\}$ couplings have been discussed in the literature. Starting from a formal theory of flexopolarization for systems described in terms of $\{\mathbf{Q},\mathbf{P}\}$ [19] possible equilibrium one-dimensional modulated structures were identified, both for nonchiral and intrinsically chiral materials [17]. The theory permits stabilization of N_{SB}, a few variants of N_{TB} -from weakly to strongly biaxial- and a new class of one-dimensional achiral modulated nematic structures. More

complex structures, like polar 2D hexagonal and 3D bcc analogues of blue phases, can also form [23].

Couplings between the pair of $\{\mathbf{Q},\mathbf{T}\}$ fields have been shown to generate even larger class of new phases, ranging from the tetrahedratic liquid to novel biaxial, polar, and chiral phases [21, 24, 25]. These phenomenological predictions are consistent with a few molecular level studies. In particular, Bisi et al. [26] showed that rigid C_2-symmetric molecules generate quadrupolar and octupolar terms to the Onsager's excluded volume, which is prerequisite for having biaxial and tetrahedratic ordering in the mean-field theory. Evaluation of point dispersion interactions [27] between two bent-core molecules gives mathematically similar terms [28]. Translating this to microscopic interactions we have studied a class of 3D, generalized Lebwohl-Lasher lattice dispersion models [28–30] with nearest-neighbour interactions involving quadrupolar and octupolar couplings. We considered only the maximal chirality model (MCM), where two-fold axes of $\mathbf{Q}$ and $\mathbf{T}$ coincide (*see* discussion after formula (7)). Both, molecular-field calculations and Monte Carlo computer simulations proved the formation of absolutely stable tetrahedratic, tetrahedratic nematic, and chiral tetrahedratic nematic liquids of global T_d , D_{2d} , and D_2 symmetry, respectively, in addition to the standard uniaxial and biaxial nematic phases. Here we carry out Monte-Carlo simulations for the model [29] in 2D. We show that the model exhibits spontaneous chiral symmetry breaking from an isotropic phase (I) to a nematic twist-bend-like structure, which appears to have a nanoscale cholesteric arrangement. The corresponding phase transition appears to be first-order.

3. Model

We consider the dispersion interaction potential which accounts, in an averaged way, for chirality that can be induced *e.g.* by conformational degrees of freedom. It is defined by a coupling between molecular multipole moments that have quadrupolar and octupolar parts. More specifically, we assume each molecule to consist of the point quadrupolar moment $\mathbf{Q}(\hat{\mathbf{\Omega}})$ and the molecular octupolar moment $\mathbf{T}_{\mathbf{2}}^{(\mathbf{3})}(\hat{\mathbf{\Omega}})$, which is a spherical, third-rank tensor of T_d point group symmetry. The quadrupolar tensor is given by

$$\mathbf{Q}(\hat{\mathbf{\Omega}}) = \mathbf{T}_{\mathbf{0}}^{(\mathbf{2})}(\hat{\mathbf{\Omega}}) + \lambda\sqrt{2}\mathbf{T}_{\mathbf{2}}^{(\mathbf{2})}(\hat{\mathbf{\Omega}}) \tag{10}$$

with the $D_{\infty h}$-symmetric (uniaxial) part

$$\mathbf{T}_{\mathbf{0}}^{(\mathbf{2})}(\hat{\mathbf{\Omega}}) = \sqrt{\frac{3}{2}}\left(\hat{\mathbf{c}}\otimes\hat{\mathbf{c}} - \frac{1}{3}\mathbb{I}\right) \tag{11}$$

and the D_{2h}-symmetric biaxial part

$$\mathbf{T}_{\mathbf{2}}^{(\mathbf{2})}(\hat{\mathbf{\Omega}}) = \frac{1}{\sqrt{2}}\left(\hat{\mathbf{a}}\otimes\hat{\mathbf{a}} - \hat{\mathbf{b}}\otimes\hat{\mathbf{b}}\right). \tag{12}$$

The right-handed molecular basis $\hat{\mathbf{\Omega}} = (\hat{\mathbf{a}},\hat{\mathbf{b}},\hat{\mathbf{c}})$ is specified by three orthonormal vectors firmly attached to the molecule and fixed parallel to two-fold axes of $\mathbf{Q}$ and $\mathbf{T}_{\mathbf{2}}^{(\mathbf{3})}$. That is, the configuration of multipoles corresponds to MCM introduced in the previous section (7). Parameter λ controls molecular biaxiality. In particular, Eq. (3) now reads

$$w = \frac{1-6\lambda^2}{(2\lambda^2+1)^{3/2}}. \tag{13}$$

The eigenvalues of $\mathbf{Q}$ corresponding to eigenvectors $(\hat{\mathbf{a}}, \hat{\mathbf{b}}, \hat{\mathbf{c}})$ are $\left(\lambda - \frac{1}{\sqrt{6}}, -\lambda - \frac{1}{\sqrt{6}}, \sqrt{\frac{2}{3}}\right)$, respectively.

The octupolar (T_d-symmetric) tensor reads

$$\mathbf{T_2^{(3)}}(\hat{\mathbf{\Omega}}, \mathbf{p}) = \frac{p}{\sqrt{6}} \sum_{(\hat{\mathbf{x}},\hat{\mathbf{y}},\hat{\mathbf{z}})\in\pi(\hat{\mathbf{a}},\hat{\mathbf{b}},\hat{\mathbf{c}})} \hat{\mathbf{x}} \otimes \hat{\mathbf{y}} \otimes \hat{\mathbf{z}}, \tag{14}$$

where summation runs over all permutations of the molecular basis and where $p = \pm 1$ is the parity degree of freedom [29]. We can correlate p with *e.g.* conformational chirality by noting that all chemically *achiral* molecules that form stable N_{TB} can be found in chiral configurations which fluctuate equally between positive and negative chiralities. To account for such chirality fluctuations we need at least one additional degree of freedom per molecule, here denoted p, which allows to distinguish between the two classes of molecular conformations of opposite chirality. To both of these classes there may correspond many conformational states of a molecule, but we assume that they do not modify the norm and relative orientation of quadrupolar and octupolar moments of each class in an essential way.

For the model considered the two opposite chiralities are realized when reflections of the molecular basis that do not preserve handedness are included. A parity flip amounts to inverting one or more of the molecular axes or, equivalently, changing the sign of $\mathbf{T_2^{(3)}}$. It modifies $\mathbf{T_2^{(3)}}$ in accordance with Eq. (14), but leaves $\mathbf{Q}$ unaffected.

The role of $\mathbf{Q}$ and $\mathbf{T_2^{(3)}}$ multipoles in chiral symmetry breaking is further illustrated in Fig.1 where symmetry of $\mathbf{Q}$ is represented by a cuboid and that of $\mathbf{T_2^{(3)}}$ by a tetrahedron. Separately, cuboid and tetrahedron are achiral, because cuboid (tetrahedron) and its mirror image can be superimposed by applying a translation and a proper rotation. However, when they are coupled by fixing mutual orientation of their two-fold axes this is not true, in general. Clearly, for the case of MCM, where two-fold axes are kept parallel as shown in Fig.1, the configuration is chiral. But, if we replace the cuboid with a cylinder, representing uniaxial symmetry, the chirality is lost, in agreement with Eq. (5). Taking all the above considerations into account we can now construct

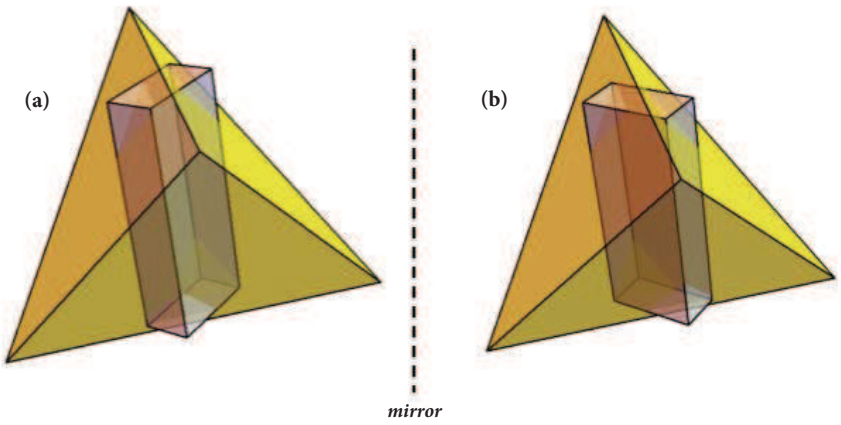

Figure 1. Maximal chirality model represented by a combination of tetrahedron and cuboid (a), where their two-fold symmetry axes are kept parallel to each other. Note that mirror image (b) of (a) cannot be brought into coincidence with (a) using translations and proper rotations. When tetrahedrons are made to coincide, cuboids are misaligned and *vice versa*.

a lattice dispersion model that allows to study a possibility of chirality fluctuations due to *e.g.*

conformational degrees of freedom. It is defined by the Hamiltonian [28–30]

$$H = \frac{1}{2} \sum_{<i,j>}^{N} \left[V(p_i, \hat{\mathbf{\Omega}}_\mathbf{i}, p_j, \hat{\mathbf{\Omega}}_\mathbf{j}) + V_c(p_i, \hat{\mathbf{\Omega}}_\mathbf{i}, p_j, \hat{\mathbf{\Omega}}_\mathbf{j}) \right]. \tag{15}$$

The sum in (15) runs over nearest neighbours, i.e. for each particle i the sum runs over z = 6 neighbouring particles j, while the N particles occupy sites of a simple cubic lattice with periodic boundary conditions. The arguments $\hat{\mathbf{\Omega}}_\mathbf{i}$ and $\hat{\mathbf{\Omega}}_\mathbf{j}$ denote the right-handed molecular frames of reference for molecules i and j, respectively, while $p_i = \pm 1$ and $p_j = \pm 1$ take into account parity of the molecular conformations.

The pair dispersion potential between neighbouring molecules involves two terms. The first one is given by

$$V(p_i, \hat{\mathbf{\Omega}}_\mathbf{i}, p_j, \hat{\mathbf{\Omega}}_\mathbf{j}) = -\epsilon \left[\mathbf{Q}(\hat{\mathbf{\Omega}}_\mathbf{i}) \cdot \mathbf{Q}(\hat{\mathbf{\Omega}}_\mathbf{j}) + \tau \mathbf{T}^{(\mathbf{3})}_\mathbf{2}(p_i, \hat{\mathbf{\Omega}}_\mathbf{i}) \cdot \mathbf{T}^{(\mathbf{3})}_\mathbf{2}(p_j, \hat{\mathbf{\Omega}}_\mathbf{j}) \right]. \tag{16}$$

It represents the interaction between quadrupolar [31] and octupolar [20] moments at sites i and j, where the scalar product ' $\cdot$ ' is understood as a full contraction over Cartesian indices.

The second term, denoted V_c , represents the lowest order coupling involving quadrupolar and octupolar moments, and the intermolecular unit vector $\hat{\mathbf{r}}_{ij}$. It reads [29]

$$V_c(p_i, \hat{\mathbf{\Omega}}_\mathbf{i}, p_j, \hat{\mathbf{\Omega}}_\mathbf{j}) = \frac{\kappa}{\epsilon} \left[\Theta_{\alpha\beta\gamma}(\hat{\mathbf{\Omega}}_\mathbf{i}) Q_{\alpha\nu}(\hat{\mathbf{\Omega}}_\mathbf{i}) Q_{\beta\nu}(\hat{\mathbf{\Omega}}_\mathbf{j}) - \Theta_{\alpha\beta\gamma}(\hat{\Omega}_j) Q_{\alpha\nu}(\hat{\mathbf{\Omega}}_\mathbf{j}) Q_{\beta\nu}(\hat{\mathbf{\Omega}}_\mathbf{i}) \right] (\hat{\mathbf{r}}_\mathbf{ij})_\gamma, \tag{17}$$

where $\Theta_{\alpha\beta\gamma}$ is given by

$$\Theta_{\alpha\beta\gamma}(p_i, \hat{\mathbf{\Omega}}_\mathbf{i}) = 2\sqrt{2} \sum_{(x,y,z)\in c(\alpha,\beta,\gamma)} T^{(2)}_{0,x\mu}(\hat{\mathbf{\Omega}}_\mathbf{i}) T^{(2)}_{2,y\nu}(\hat{\mathbf{\Omega}}_\mathbf{i}) T^{(3)}_{2,\mu\nu z}(p_i, \hat{\mathbf{\Omega}}_\mathbf{i}). \tag{18}$$

Here summation runs over cyclic permutations $c(\alpha, \beta, \gamma)$ of $\{\alpha, \beta, \gamma\}$. It is perhaps worthwhile to add that terms similar to (16-18) can be generated by considering multipole expansion of the Onsager's excluded volume between two bent-core molecules in chiral conformations. The only difference would be additional polar couplings, which we disregarded here.

Special cases of the model (15) have already been studied. For $\tau = \lambda = \kappa = 0$ the model reduces to the Lebwohl-Lasher [32] potential, which accounts for isotropic and uniaxial nematic phases connected by a first-order phase transition. Luckhurst *et al.* considered $\tau = \kappa = 0$ case [31, 33] with nonzero λ parameter, which controls the biaxiality of a molecule. For $0 \leq \lambda \leq \sqrt{\frac{3}{2}}$ the parameter w, Eq. (13), covers the whole interval of allowed values approaching maximal biaxiality case ($w = 0$) at the so called self-dual point ($\lambda = 1/\sqrt{6}$), where molecules are neither prolate nor oblate. The self-dual point separates phases in which the biaxial molecules are prolate-like ($\lambda < 1/\sqrt{6}$) from phases in which the molecules are oblate-like ($\lambda > 1/\sqrt{6}$), while the boundary cases correspond to Maier-Saupe-like uniaxial models for long rods ($\lambda = 0$) and platelets ($\lambda = \sqrt{\frac{3}{2}}$). The phase diagram for varying λ has been obtained using mean-field theory and confirmed by Monte Carlo simulations [34]. The model predicts a prolate uniaxial nematic phase, an oblate uniaxial nematic phase, a biaxial nematic phase, and an isotropic phase, where a sequence of a first-order transition to the uniaxial nematic and second-order transition to the biaxial nematic occurs with lowering temperature. At $\lambda = 1/\sqrt{6}$ only a direct transition from the isotropic to the biaxial nematic phase takes place.

When only the octupolar coupling term, proportional to $\epsilon\tau$ is retained in Eq. (16), the model predicts first-order transition from the isotropic phase to the tetrahedratic phase of T_d symmetry and was studied by Romano [35] and by one of us [28, 29]. A full analysis of the model when $\kappa = 0$ is

given in [28, 29]. We identified, in addition to the uniaxial, biaxial and tetrahedratic nematic phases, two further spatially homogeneous nematic like phases. They involved nematic tetrahedratic and chiral nematic tetrahedratic phases of global D_{2d}, and D_2 symmetry, respectively.

For the most complex case, where additionally $\kappa \neq 0$, only preliminary results are available [29, 30]. Such coupling, as we showed, can superimpose spatially inhomogeneous (short or long-range) orientational order on the structures already identified. In particular, the chiral nematic tetrahedratic phase becomes unstable against spontaneous twist formation. Indeed, by considering the minimum of the interaction potential for two isolated neighbouring molecules we find that it favours a locally twisted configuration with pitch being of the order of $\pi(\Lambda + 4\tau)/(\kappa\Lambda\overline{p})$, where $\Lambda = 3 + 2\lambda(\sqrt{6} + \lambda)$ and where $\overline{p}$ is the average parity ($\overline{p} = 1$ or $\overline{p} = -1$ for biaxial molecules in the ground state)[29]. In other words, both for phases with $\overline{p} \neq 0$ and with $\overline{p} = 0$, twisted domains of opposite handedness will form in equal abundance, leading to ambidextrous chirality.

An important phenomenon associated with a formation of spontaneous twist in the model (15) is *frustration* of orientational order. This is illustrated in Fig. (2), where three biaxial molecules are placed in the $(\hat{\mathbf{x}}, \hat{\mathbf{y}})$ plane with the intermolecular vectors constrained to four directions $\hat{\mathbf{r}}_{ij} = \{1, 0\}, \{0, 1\}, \{-1, 0\}, \{0, -1\}$. Consider now that two molecules, 1 and 2, of identical parity $p_1 = p_2 = +1$, occupy neighbouring sites at positions $(x_1, y_1) = (0, 0)$ and $(x_2, y_2) = (1, 0)$ (Fig. 2a). As discussed above, the ground state of such configuration is achieved when both molecules 1 and 2 align with $\hat{\mathbf{a}}_1 \parallel \hat{\mathbf{a}}_2 \parallel \hat{\mathbf{r}}_{12} = \{1, 0\}$ and molecule 2 is tilted clockwise with respect to 1 around $\hat{\mathbf{a}}_2$ (or vice-versa). Now consider a third molecule, 3, $p_3 = p_1 = p_2 = +1$, located at $(x_3, y_3) = (0, 1)$. If 1 and 3 were treated in isolation (Fig. 2b), their ground state configuration would be achieved analogously, by aligning $\hat{\mathbf{a}}_3 \parallel \hat{\mathbf{a}}_1 \parallel \hat{\mathbf{r}}_{13}$ and tilting 3 clockwise with respect to 1 along $\hat{\mathbf{a}}_3$ (or vice-versa). Now notice that the two pairwise ground states for 1 and 2 and for 1 and 3 cannot be achieved simultaneously (Fig. 2c). Adding more molecules multiplies the number of conflicting conditions. Thus, the system is frustrated. The question of how the system can relax frustrated configurations is difficult to answer on analytical grounds and in the present we resort to Monte Carlo simulation in search for an answer in 2D. The 3D case is postponed to our forthcoming studies. We demonstrate that the 2D MCM model releases frustration by a first- order, isotropic-ambidextrous cholesteric phase transition. The obtained ambidextrous cholesteric phase (N_A^*) can be regarded as the limiting case of N_{TB}, where the director tilts at right angle with respect to the helix axis.

4. Results and conclusions

We perform Monte-Carlo simulations of a system of molecules interacting with the hamiltonian (15) on a two dimensional, square grid with periodic boundary conditions in the lattice plane and free boundary conditions in the perpendicular direction. Two different sample sizes are used: 32×32 and 64×64 to ensure that finite size effects are kept under the control. We take $\kappa = \tau = 1.0$, $0.1 \lesssim \lambda \lesssim 0.9$ and use the dimensionless, reduced temperature $t = k_B T/\epsilon$ for temperature scans. If not stated othervise simulations for different temperatures are initialized from a random, disordered state. In each Metropolis step a random site in the grid is selected. Each attempted MC move involves proper random rotation (generated using quaternions) of the molecular frame and parity inversion. Whenever possible, the size of the MC rotational step is adjusted to give acceptance ratio at the level of $0.3 - 0.5$.

The thermalization process is system's size dependent and lasts, on the average, for about 10^5 cycles. After thermalization, the production run involves 10^5 cycles with every tenth cycle configuration taken to calculate thermodynamic averages. Typical final configurations of the production run for $\lambda = 0.3$ are shown in Fig. 3, where the transition between I and N_A^* is observed at $t^* = 0.888 \pm 0.001$. As expected, for $t > t^*$ the isotropic structure is stabilized where small, orientationally ordered domains representing both chiralities are present. For temperatures slightly below the phase transition the system becomes orientationally ordered and chiral, with the main direc-

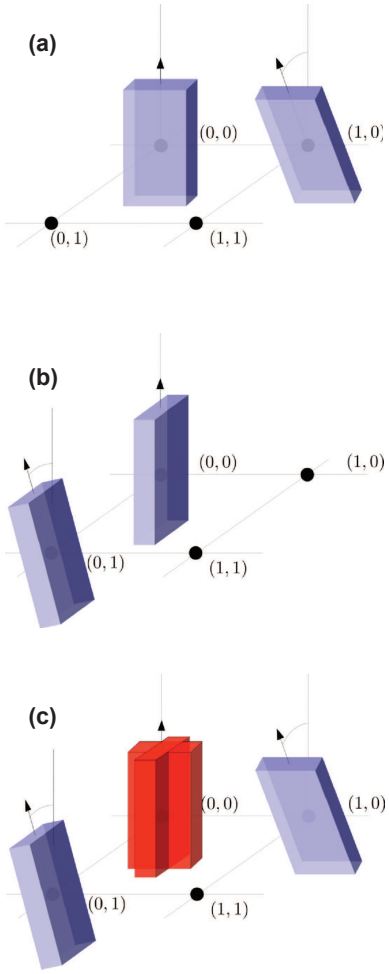

Figure 2. Illustration of how frustration emerges for $\kappa \neq 0$ (18) when three instead of two biaxial molecules with identical parity ($p = +1$) are considered. Molecules are represented by cuboids, which roughly correspond to the molecular quadrupolar tensors $\mathbf{Q}(\hat{\mathbf{\Omega}})$: a) Ground state of two isolated molecules placed on neighbouring lattice sites along $\hat{\mathbf{x}}$. b) Ground state of two isolated molecules placed on neighbouring lattice sites along $\hat{\mathbf{y}}$. c) The two pairwise ground states (a) and (b) conflict each other.

tor perpendicular to the modulation axis. Because of a random initial state, chiral ambidextrous domains can form below t^* as shown in Fig. 3(d).

The phase transition to N_A^* is found by monitoring the average energy per molecule, the specific heat and the parity order parameter

$$\overline{p} = \overline{\frac{1}{N}\sum_{i=1}^{N} p_i}, \tag{19}$$

where overline denotes thermodynamic average. Exemplary temperature dependence of the average energy, the heat capacity and the parity order parameter for $\lambda = 0.3$ are shown in Fig.4. Similar

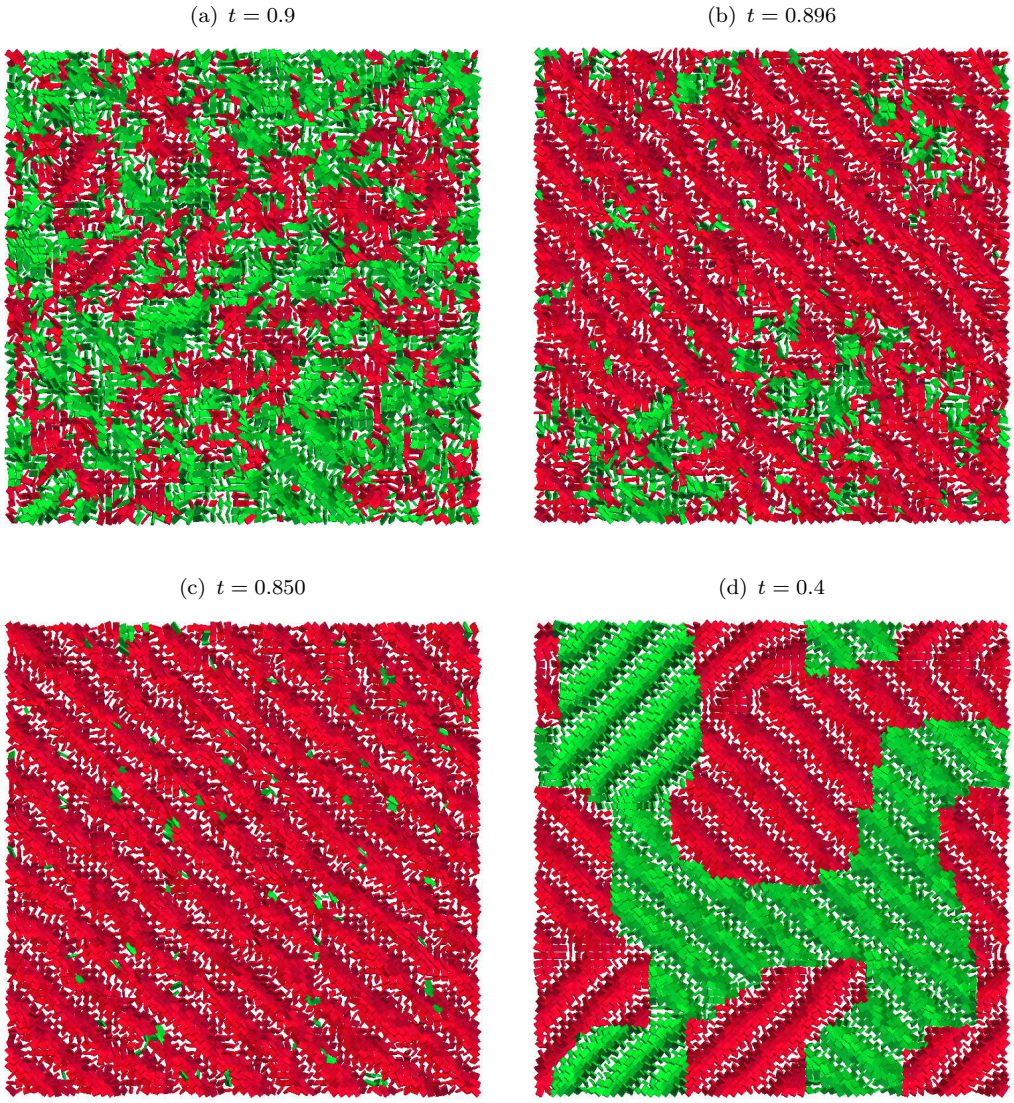

Figure 3. Exemplary snapshots of equilibrium configurations on 64×64 lattice for $\lambda = 0.3$, $\tau = \kappa = 1$, and for different temperatures t, showing disordered and ordered structures. Sides of cuboids are moduli of eigenvalues of the $\mathbf{Q}$ tensor, while the color represents parity: $p = +1$ (red) and $p = -1$ (green). The phase transition temperature is $t^* = 0.888 \pm 0.001$. Simulations were initialized from a random parity distribution and orientationaly disordered configuration of molecular tripods.

plots are obtained both for 32×32 and 64×64 systems indicating that finite size effects are kept within the statistical error. The average energy and the parity order parameter show a jump at $t^* \approx 0.888$ suggesting that the phase transition is of the first order. As the heat capacity is peaked around the same temperature the peak's position is used to determine the transition temperature. With this identification of the phase transition temperature a detailed analysis of t^* as function of λ is given in Fig. 5. It shows that t^* increases with increasing λ.

A further support for the first-order nature of the $I - N_A^*$ phase transition is the observation of hysteresis for the average parity (19), as shown in Fig. 6. More specifically, when the temperature scan, starting from a random initial configuration in high temperature phase, progresses by cooling down in small temperature steps to the final ordered state at low temperature and then is heated up until temperature of the high temperature state is reached again, the average parities obtained from the corresponding production runs on cooling and heating are slightly shifted.

To perform detailed structure analysis of low temperature phase we equilibriate monodomains of definite chirality, like the one shown in Fig.7(a), and study average orientational properties of the molecular tripods $\{\hat{\mathbf{a}}_i, \hat{\mathbf{b}}_i, \hat{\mathbf{c}}_i\}$, Fig.7(b). Calculation of the average direction of these vectors shows

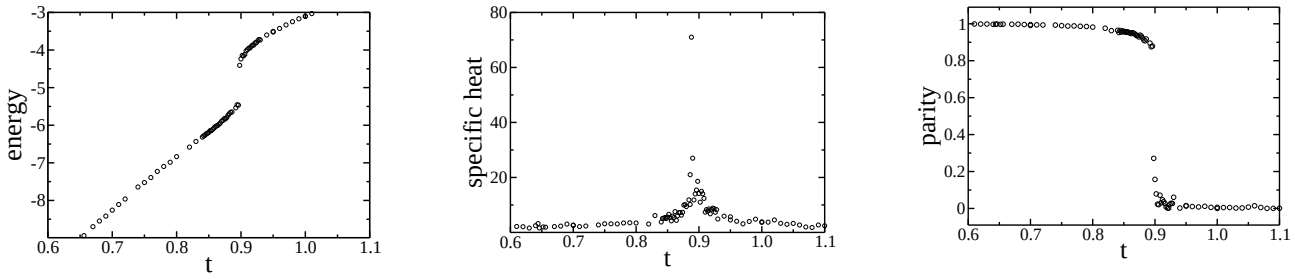

Figure 4. Temperature dependence of (a) energy, (b) specific heat, and (c) average parity for $\lambda = 0.3$ and $\tau = \kappa = 1$, calculated for equilibrium configurations on 32×32 lattice. Each dot correspond to an equilibrium value obtained from independent MC simulation started from randor

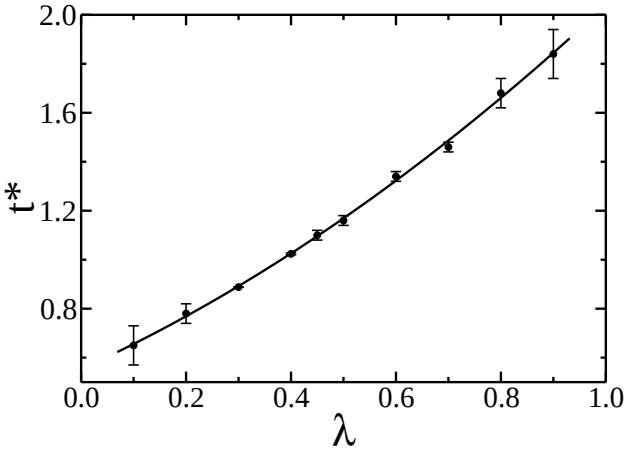

Figure 5. Transition temperatures for $0.1 \leq \lambda \leq 0.9$ estimated from a position of the peak in specific heat dependence on t. Error bars correspond to the width of the peak. The system's size is 32×32 and $\tau = \kappa = 1$. Dots are data obtained from simulations; solid line is to gu

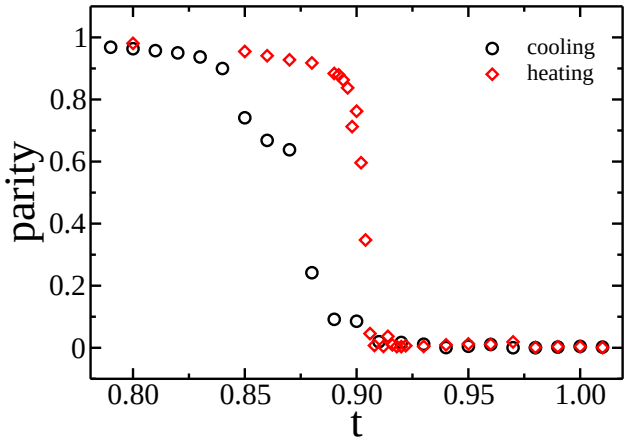

Figure 6. Parity dependence on t for $\lambda = 0.3$, $\tau = \kappa = 1$ when 64×64 sample was heated (squares) and cooled (diamonds). Presence of considerable jump and hysteresis suggests that the transition is of the first order.

that only one of them, $\hat{\mathbf{a}} = \overline{\hat{\mathbf{a}}_i}$, does not vanish. The other two rotate around the $\mathbf{k}$-axis, which is parallel to $\hat{\mathbf{a}}$, Fig.7(b). This behaviour is typical for cholesteric ordering with the cholesteric pitch, being in the studied case equal to $\pi/0.66 = 4.76$. Similar analysis can be carried out for cholesteric phases obtained for different values of λ. The corresponding cholesteric pitch is shown in Fig.8. Note that the pitch decreases with λ.

Summarizing, we showed that the coupling between quadrupolar and octupolar interactions can lead to chiral symmetry breaking in 2D with orientational arrangement similar to that observed

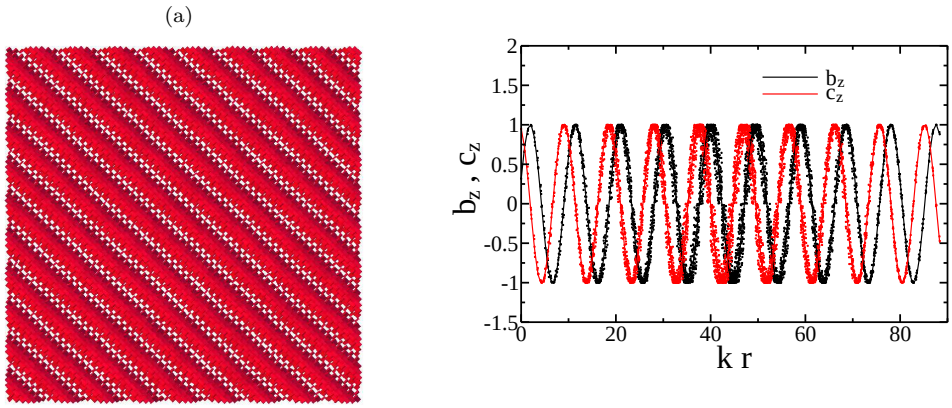

Figure 7. Exemplary (a) snapshot of equilibrium monodomain configuration of parity $\overline{p} \approx +1$ for $\lambda = 0.3$, $\tau = \kappa = 1$ and for very low temperature $t = 0.05$. Sides of cuboids are moduli of eigenvalues of the $\mathbf{Q}$ tensor. (b) The corresponding z-components of $\hat{\mathbf{b}} = \overline{\hat{\mathbf{b}}_i}$ and $\hat{\mathbf{c}} = \overline{\hat{\mathbf{c}}_i}$ as function of position $\mathbf{r}$ along the modulation axis $\mathbf{k} \parallel \hat{\mathbf{a}} = [0.681, 0.732, 0.]$. Dots are data calculated for the snapshot (a) and lines are least-square fits: $b_z(\mathbf{k}\cdot\mathbf{r}) = \sin(0.660\,\mathbf{k}\cdot\mathbf{r} + 0.318)$ and $c_z(\mathbf{k}\cdot\mathbf{r}) = \sin(0.660\,\mathbf{k}\cdot\mathbf{r} + 1.879)$.

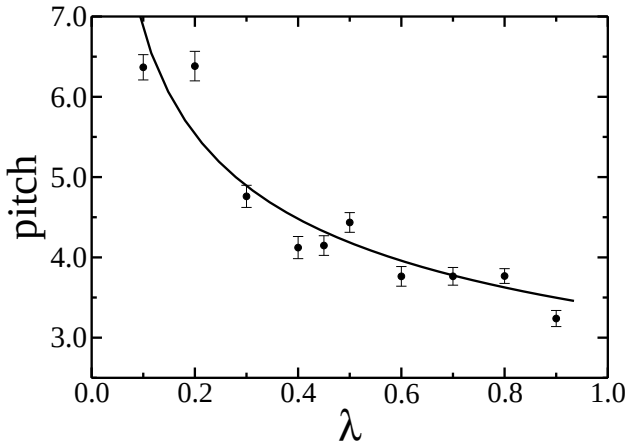

Figure 8. Pitch of low temperature ambidextrous cholesteric phase as function of λ for $\tau = \kappa = 1$. Dots are data from simulations. The error bars are due to finite size of the system. Solid line is to guide the eye.

for N_{TB} in 3D. Although in two dimensions we do not expect any spontaneous breakdown of continuous symmetries the introduced molecular parity is a discrete, Ising-like molecular degree of freedom and the MCM hamiltonian (15) is $Z(2) \times SO(3)$ symmetric. Hence, it is not unreasonable to expect that a phase transition involving spontaneous parity (chirality) breaking can occur even in 2D. Indeed, as we demonstrated the new ambidextrous cholesteric phase can be stabilized from the isotropic phase through the first order phase transition for the MCM model. This structure apparently relaxes the frustration, Fig. 2, of the hamiltonian‘s ground state and is remarkably stable as seen from Fig 4(c).

The results of simulations indicate that the complex effects due to spontaneous breaking of chirality, encountered *e.g.* in bent-core and flexible dimer systems can be accounted for in a microscopic dispersion model with couplings such as (15). Subsequent, detailed analysis needs to be undertaken to study the phase transitions and remaining unidentified structures, which can exist in the three-dimensional case. Finally, because geometrical frustration and chirality are known to lead to the emergence of blue phases, it is important to establish whether a link between the model (15) to those structures exists.

Acknowledgements

This work was supported by Grant No. DEC-2013/11/B/ST3/04247 of the National Science Centre in Poland.

References

[1] Panov V, Nagaraj M, Vij J, Panarin YP, Kohlmeier A, Tamba M, Lewis R, Mehl G. Spontaneous periodic deformations in nonchiral planar-aligned bimesogens with a nematic-nematic transition and a negative elastic constant. Phys Rev Lett. 2010;105(16):167801.

[2] Cestari M, Diez-Berart S, Dunmur D, Ferrarini A, de La Fuente M, Jackson D, Lopez D, Luckhurst G, Perez-Jubindo M, Richardson R, Salud J, Timimi B, Zimmermann H. Phase behavior and properties of the liquid-crystal dimer 1, 7-bis (4-cyanobiphenyl-4-yl) heptane: A twist-bend nematic liquid crystal. Phys Rev E. 2011;84(3):031704.

[3] Borshch V, Kim YK, Xiang J, Gao M, Jákli A, Panov VP, Vij JK, Imrie CT, Tamba MG, Mehl GH, et al. Nematic twist-bend phase with nanoscale modulation of molecular orientation. Nat Commun. 2013;4.

[4] Chen D, Porada JH, Hooper JB, Klittnick A, Shen Y, Tuchband MR, Korblova E, Bedrov D, Walba DM, Glaser MA, et al. Chiral heliconical ground state of nanoscale pitch in a nematic liquid crystal of achiral molecular dimers. PNAS. 2013;110(40):15931–15936.

[5] Yoshizawa A, Kato Y, Sasaki H, Takanishi Y, Yamamoto J. Chiral conglomerates observed for a binary mixture of a nematic liquid crystal trimer and 6ocb. Soft Matter. 2015;11(45):8827–8833.

[6] Görtz V, Southern C, Roberts NW, Gleeson HF, Goodby JW. Unusual properties of a bent-core liquid-crystalline fluid. Soft Matter. 2009;5(2):463–471.

[7] Chen D, Nakata M, Shao R, Tuchband MR, Shuai M, Baumeister U, Weissflog W, Walba DM, Glaser MA, Maclennan JE, et al. Twist-bend heliconical chiral nematic liquid crystal phase of an achiral rigid bent-core mesogen. Phys Rev E. 2014;89(2):022506.

[8] Wang Y, Singh G, Agra-Kooijman DM, Gao M, Bisoyi HK, Xue C, Fisch MR, Kumar S, Li Q. Room temperature heliconical twist-bend nematic liquid crystal. CrystEngComm. 2015;17(14):2778–2782.

[9] de Gennes PG, Prost J. The physics of liquid crystals. Clarendon Press, Oxford; 1995.

[10] Greco C, Luckhurst GR, Ferrarini A. Molecular geometry, twist-bend nematic phase and unconventional elasticity: a generalised maier–saupe theory. Soft Matter. 2014;10(46):9318–9323.

[11] Greco C, Ferrarini A. Entropy-driven chiral order in a system of achiral bent particles. Phys Rev Lett. 2015;115(14):147801.

[12] Tschierske C, Ungar G. Mirror symmetry breaking by chirality synchronisation in liquids and liquid crystals of achiral molecules. ChemPhysChem. 2016;17(1):9–26.

[13] Dozov I. On the spontaneous symmetry breaking in the mesophases of achiral banana-shaped molecules. EPL. 2001;56(2):247.

[14] Meyer RB. Piezoelectric effects in liquid crystals. Phys Rev Lett. 1969;22(18):918.

[15] Mayer RB. Proceedings of the les houches summer school on theoretical physics, 1973, session no. xxv. Gordon and Breach; 1976. p. 271–343.

[16] Shamid SM, Dhakal S, Selinger JV. Statistical mechanics of bend flexoelectricity and the twist-bend phase in bent-core liquid crystals. Phys Rev E. 2013;87(5):052503.

[17] Longa L, Pajak G. Modulated nematic structures induced by chirality and steric polarization. Phys Rev E. 2016 Apr;93:040701; Available from: `http://link.aps.org/doi/10.1103/PhysRevE.93.040701`.

[18] Allender D, Longa L. Landau–de gennes theory of biaxial nematics reexamined. Phys Rev E. 2008; 78(1):011704.

[19] Longa L, Trebin HR. Spontaneous polarization in chiral biaxial liquid crystals. Phys Rev A. 1990 Sep; 42:3453–3469; Available from: `http://link.aps.org/doi/10.1103/PhysRevA.42.3453`.

[20] Fel L. Symmetry of the fréedericksz transition in nonchiral nematic liquid crystals. Phys Rev E. 1995; 52(3):2692.

[21] Lubensky T, Radzihovsky L. Theory of bent-core liquid-crystal phases and phase transitions. Phys Rev E. 2002;66(3):031704.

[22] Longa L, Fink W, Trebin HR. Biaxiality of chiral liquid crystals. Phys Rev E. 1994;50(5):3841.

[23] Shamid SM, Allender DW, Selinger JV. Predicting a polar analog of chiral blue phases in liquid crystals. Phys Rev Lett. 2014;113(23):237801.
[24] Brand HR, Pleiner H, Cladis P. Tetrahedratic cross-couplings: novel physics for banana liquid crystals. Physica A: Statistical Mechanics and its Applications. 2005;351(24):189 – 197; Available from: http://www.sciencedirect.com/science/article/pii/S0378437104015778.
[25] Brand HR, Pleiner H. Macroscopic behavior of non-polar tetrahedratic nematic liquid crystals. The European Physical Journal E. 2010;31(1):37–50; Available from: http://dx.doi.org/10.1140/epje/i2010-10547-9.
[26] Bisi F, Longa L, Pajak G, Rosso R. Excluded-volume short-range repulsive potential for tetrahedral molecules. Molecular Crystals and Liquid Crystals. 2010;525(1):12–28; Available from: http://dx.doi.org/10.1080/15421401003795670.
[27] Buckingham AD. Theory of long-range dispersion forces. Discuss Faraday Soc. 1965;40:232–238; Available from: http://dx.doi.org/10.1039/DF9654000232.
[28] Longa L, Pajak G, Wydro T. Chiral symmetry breaking in bent-core liquid crystals. Phys Rev E. 2009; 79(4):040701.
[29] Trojanowski K, Pajak G, Longa L, Wydro T. Tetrahedratic mesophases, chiral order, and helical domains induced by quadrupolar and octupolar interactions. Phys Rev E. 2012;86(1):011704.
[30] Trojanowski K, Longa L. Ambidextrous chiral domains in nonchiral liquid-crystalline materials. Acta Phys Polon B. 2013;44(5):1201–1208.
[31] Luckhurst G, Zannoni C, Nordio P, Segre U. A molecular field theory for uniaxial nematic liquid crystals formed by non-cylindrically symmetric molecules. Molecular Physics. 1975;30(5):1345–1358; Available from: http://dx.doi.org/10.1080/00268977500102881.
[32] Lebwohl PA, Lasher G. Nematic-liquid-crystal order¯a monte carlo calculation. Phys Rev A. 1972 Jul; 6:426–429; Available from: http://link.aps.org/doi/10.1103/PhysRevA.6.426.
[33] Luckhurst G, Romano S. Computer simulation studies of anisotropic systems. Molecular Physics. 1980; 40(1):129–139; Available from: http://dx.doi.org/10.1080/00268978000101341.
[34] Biscarini F, Chiccoli C, Pasini P, Semeria F, Zannoni C. Phase diagram and orientational order in a biaxial lattice model: A monte carlo study. Phys Rev Lett. 1995 Aug;75:1803–1806; Available from: http://link.aps.org/doi/10.1103/PhysRevLett.75.1803.
[35] Romano S. Computer simulation study of a simple tetrahedratic mesogenic lattice model. Phys Rev E. 2008 Feb;77:021704; Available from: http://link.aps.org/doi/10.1103/PhysRevE.77.021704.

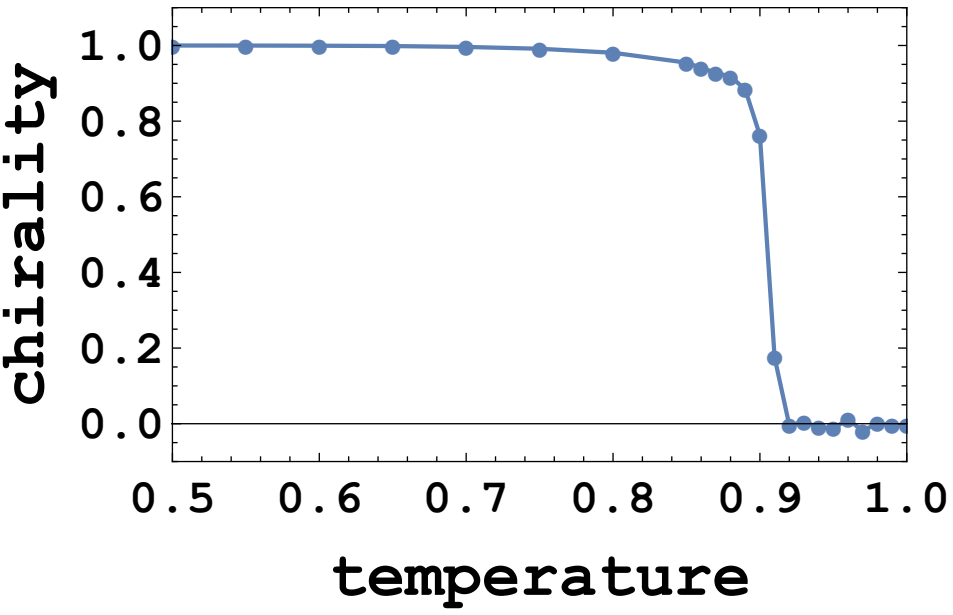
chirality
1.0
0.8
0.6
0.4
0.2
0.0
0.5
0.6
0.7
0.8
0.9
1.0
temperature